ELSEVIER

Journal of Chromatography A, 794 (1998) 327–344

JOURNAL OF CHROMATOGRAPHY A

Characterization of protein glycoforms by capillary-zone electrophoresis–nanoelectrospray mass spectrometry

Kevin P. Bateman[a,b], Robert L. White[a], Makoto Yaguchi[c], Pierre Thibault[b,*]

[a]*Department of Chemistry, Dalhousie University, Halifax, Nova Scotia B3H 4J3, Canada*
[b]*Institute for Marine Biosciences, NRC, Halifax, Nova Scotia B3H 3Z1, Canada*
[c]*Institute for Biological Sciences, NRC, Ottawa, Ontario K1A 0R6, Canada*

Abstract

The investigation of N- and O-linked glycoproteins using capillary-zone electrophoresis interfaced with nanoelectrospray mass spectrometry is described. The combination of high-resolution separation with high-sensitivity mass spectrometric detection provides analysis of glycoprotein digests at sample loadings of high femtomoles to low picomoles. Stepped-orifice voltage scanning is used to identify glycopeptides in complex proteolytic digests. Further structural information is obtained using capillary zone electrophoresis (CZE)–MS–MS to elucidate the composition of both N- and O-linked glycopeptide oligosaccharides. Collisional activation in the orifice/skimmer region is used to generate first-generation fragment ions which undergo subsequent dissociation in the r.f.-only collision cell of the triple quadrupole mass spectrometer. These experiments provided informative peptide backbone fragment ions usually not available from fragment ion spectra of multiply protonated glycopeptide ions. These methods were applied to the characterization of α-amylase inhibitor 1, a lectin from *Lotus tetragonolobus*, two N-linked glycoproteins, and to κ-casein, a glycoprotein comprising O-linked sialylated glycans.

Keywords: Mass spectrometry; Glycoproteins; 1-α-Amylase inhibitor; Caseins

1. Introduction

The covalent attachment of oligosaccharides to proteins is one of the most common post-translational modifications of eukaryote cells. Glycoproteins are fundamental to many important biological processes, including fertilization, immune defense, viral replication, parasitic infection, cell growth, cell–cell adhesion, degradation of blood clots, and inflammation [1]. These biomolecules contain oligosaccharides that are attached to a protein at the hydroxyl group of serine or threonine (O-linked) or to the amide sidechain of asparagine (N-linked). Variable oligosaccharide structures can be found at each linkage site, and further complexity arises from the partial occupancy at each glycosylation site. As a consequence of this microheterogeneity, a glycoprotein occurs in nature as a set of glycosylated variants referred to as glycoforms [2], rather than a single structural entity. The N-linked glycoproteins can be divided into three main categories: high-mannose, hybrid, and complex [3,4]. All three types share a common pentasaccharide core, $Man_3GlcNAc_2$, and are attached to the asparagine residue of the polypeptide chain via the reducing end GlcNAc. The core of N-linked oligosaccharides originates from a common precursor oligosaccharide, $Glc_3Man_9GlcNAc_2$ [3,4]. This oligosaccharide precursor is assembled in the endoplasmic reticulum on an isoprenoid lipid,

*Corresponding author. Institute for Biological Sciences, 100 Sussex Drive, Ottawa, Ontario, Canada.

0021-9673/98/$19.00
PII S0021-9673(97)00937-0

dolicholpyrophosphate, and then transferred to the growing polypeptide chain. Cleavage of the non-reducing end saccharide residues results in the formation of the high-mannose-type oligosaccharides. The complex oligosaccharides are produced by first trimming the precursor oligosaccharide even further to generate the pentasaccharide core, followed by the biosynthetic incorporation of different residues such as galactose, glucose, GlcNAc, sialic acid and fucose by glycosyl transferases. This process occurs as the glycoprotein travels through the various compartments of the Golgi complex [3,4]. Hybrid oligosaccharides encompass features of both high-mannose and complex types. N-linked glycosylation generally occurs at the sequon Asn–X–Ser or Asn–X–Thr, where X is any amino acid except proline [5–7]. Recently, it has been shown the amino acid at the X position plays a role in glycosylation efficiency at that sequon [8].

In contrast, O-linked glycoproteins do not share a common core structure. They can be categorized into at least six different groups according to core structures [1]. Although the oligosaccharides are often linked to serine or threonine residues through a GalNAc residue, the linkages may also involve other residues. The synthesis of O-linked oligosaccharides is entirely a post-translational event with a series of enzymes acting sequentially on the fully folded protein. Unlike N-linked glycosylation, no signal sequon has yet been found for O-linked glycosylation. Since not all hydroxyamino acids are O-glycosylated, signals must exist to specify which Ser and Thr residues acquire O-glycans. Charged amino acids in the proximity of the sites of glycosylation may play an important role in signaling this post-translational modification [9].

The complexity of glycoproteins provides for a truly challenging analytical problem. Various approaches have been developed for the characterization of both the carbohydrate structure and the sequence of the protein. All carbohydrates appended to the protein structure can be removed chemically or enzymatically and collected as a pool of mixed oligosaccharides. These are then analyzed by various methods, including NMR spectroscopy, enzymatic digestion, chemical cleavage, and methylation followed by GC–MS [10], providing information on the composition and linkages of the various sugars present in the carbohydrate. Mass spectrometry of the intact oligosaccharide provides molecular weight information, and high-energy tandem MS studies can be used to assign the structure and linkages of the oligosaccharide [11].

Protein analysis after removal of the attached carbohydrates provides the amino acid sequence of the original glycoprotein. For N-linked glycoproteins, identification of potential sites of glycosylation can be made based on the consensus sequon, although further confirmation is required. For unequivocal determination of the site of linkage, the glycoproteins are typically digested using proteolytic enzymes followed by endoglycosidases, and the resulting digests are analyzed by LC–UV or LC–MS before and after removal of the glycoforms [12,13]. The peaks which disappear in the second analysis are identified as glycopeptides, and can be reisolated from the original glycoprotein digest for further characterization using Edman sequencing. The amino acid linked to carbohydrates would typically be lost in the washing cycle, thereby resulting in a blank during the sequencing analysis. This can be further confirmed by conducting the Edman degradation of the glycopeptide after chemical or enzymatic removal of the carbohydrate.

Mass spectrometry has played a valuable role in the elucidation of glycoprotein structure, including carbohydrate structure and amino acid sequence. Recently, several MS techniques enabling the identification of glycopeptides in digests of glycoproteins have been reported [14,15]. In these methods, specific classes of carbohydrates are identified from the characteristic oxonium ions (Table 1) formed by fragmentation in the orifice/skimmer region of the

Table 1
Diagnostic oxonium ions for glycopeptides

m/z	Carbohydrate residues
133	Pentose (Ara, Rib, Xyl)
147	Deoxyhexose (Fuc)
162	Hexosamine (GalN, GlcN)
163	Hexose (Glc, Gal, Man)
204	N-Acetyl hexosamine (GalNAc, GlcNAc)
274	N-Acetyl neuramic acid–H_2O (Neu_5Ac-H_2O)
292	N-Acetyl neuramic acid (Neu_5Ac)
366	HexNAc–Hex
407	HexNAc–HexNAc

mass spectrometer. The mass spectrometer is scanned over the region corresponding to these oxonium fragment ions using a high-orifice/skimmer voltage to promote their formation prior to mass spectral analysis. The potential drop in this region is then reduced to permit transmission of the multiply protonated ions for the intact peptides and glycopeptides. By using the first of these scan functions the location of the glycopeptides in the total ion chromatogram can be determined. Once the glycopeptides have been thus identified, the relevant intact precursor ions can be subjected to LC–MS–MS analysis and further structural information on the glycoform can be obtained. Low energy collision activation of glycopeptides typically results in cleavage of the labile glycosidic bonds, while the peptide linkages do not normally dissociate in this collision regime. Although tandem mass spectra of glycopeptides provide important structural information concerning the oligosaccharide appended to the peptide this technique is of limited practical value for sequencing the peptide backbone.

Another shortcoming of the LC–MS techniques described above is the limited chromatographic resolution obtained for glycopeptides present in digests of glycoproteins. The glycopeptides tend to be present as broad peaks in the tryptic map, indicative of the microheterogeneity of these fragments [15]. CZE has greatly enhanced resolving power relative to HPLC, and this attribute has been used in the study of glycoproteins and carbohydrates ([16], and Refs. therein).

Although providing superior resolution relative to HPLC methods, CZE–MS suffers from poor concentration detection limits. Several approaches have been investigated to circumvent this limitation, including sample stacking [17,18], isotachophoresis [19], and solid-phase extraction [20]. More recently, nanoelectrospray sources have been described for CZE–MS, and were shown to provide remarkable sensitivities especially for glycoprotein analysis [21,22].

This report describes the use of nanoelectrospray CZE–MS for the study of N- and O-linked glycoprotein digests. Mixed scan functions to generate carbohydrate specific ions are used to identify glycopeptides in complex peptide maps. The high resolution obtained using CZE provides information on glycoform populations at individual sites of glycosylation, while combined tandem mass spectrometric experiments enable characterization of the oligosaccharide structures. More importantly, the present investigation highlights a novel CZE–MS–MS approach to achieve peptide sequencing using sub-picomole quantities of the original glycoproteins.

2. Experimental

2.1. Reagents and materials

All fused-silica capillaries were purchased from Polymicro Technologies (Phoenix, AZ, USA). The capillary column butt connector (part no. 2-3796) was obtained from Supelco (Oakville, Ontario, Canada). Formic acid (99%), ammonium persulfate (98%), and the *Lotus tetragonolobus* lectin were purchased from Sigma (St. Louis, MO, USA), and were used without further purification. The *Phaseolus vulgaris* α-amylase inhibitor 1 was a kind gift from Dr. Marteen Chrispeels (Dept. of Biology, University of California, San Diego, CA, USA) and was further purified using reversed-phase C_8 HPLC to isolate the 11.5-kDa α-chain glycopeptide prior to mild acid cleavage. The κ-casein was prepared according to the method of Zittle and Custer [23], with the exception that the final purification with ethanol was omitted. A 1% (w:v) solution of κ-casein in 50 m*M* Tris–citrate (pH 6.6) was treated with rennin (1 μg rennin/mg of κ-casein) for 15 min at 35°C. The pH of the solution was adjusted to 4.6 and the *para*-κ-casein was precipitated. The supernatant solution containing the soluble rennin fragment was dialysed at 4°C overnight and freeze-dried prior to proteolytic digestion. Sequencing-grade TPCK-trypsin and endoproteinase Glu-C were purchased from Boehringer MannHeim (Montreal, Quebec, Canada). 7-Oct-1-enyltrimethoxysilane was purchased from Hüls America (Bristol, PA, USA). For modification of the capillary surface, [(acryloylamino)propyl]trimethyl-ammonium chloride (referred to as BCQ by the manufacturer) was supplied by Chemische Fabrik Stockhaussen (Krefeld, Germany), and (3-aminopropyl)trimethoxysilane (APS) was obtained from Sigma. N,N,N′,N′-Tetramethylethylenediamine (TEMED) was purchased

from International Biotechnologies (New Haven, CT, USA). Sal Hyde 24K bright English gold plating salts (Mr. Clock, Halifax, Nova Scotia, Canada) were used to prepare the gold plating solution, and the silver conductive paint was purchased at a local General Motors automobile dealership.

2.2. Protein digests

2.2.1. Tryptic digests

L. tetragonolobus lectin (0.98 mg) was dissolved in 0.2 *M* ammonium bicarbonate. Tryptic digestion was carried out for 24 h at 37°C using a substrate-to-enzyme ratio of 30:1. The solution was evaporated to dryness and the residue was dissolved in deionized water to a final concentration of 4.9 mg/ml, calculated in terms of the original mass of glycoprotein.

2.2.2. Endoproteinase Glu-C digests

The κ-casein rennin fragment (2.7 mg) was dissolved in 0.2 *M* ammonium bicarbonate. Glu-C digestion was carried out for 5 h at 37°C using a substrate-to-enzyme ratio of 50:1. The solution was evaporated to dryness and the residue was dissolved in deionized water to a final concentration of 10 mg/ml, calculated in terms of the original mass of glycoprotein.

2.2.3. Mild acid cleavage

The α-chain of α-amylase inhibitor 1 (0.5 mg) was dissolved in 0.25 *M* acetic acid and incubated at 115°C for 8 h to favor cleavage at the aspartic acid residue. The digested protein solution was evaporated to dryness and the residue was redissolved in deionized water to a final concentration of 1.0 mg/ml.

2.3. Capillary coatings

Capillary was typically coated in 5-m lengths and cut as needed for use in CZE–UV or CZE–MS experiments.

2.3.1. BCQ coating

The method used for preparing the BCQ coating was described previously [22]. The capillary was rinsed sequentially with 1 *M* NaOH, deionized water and methanol, each for 1 h at 20 p.s.i. (1 p.s.i. = 6894.76 Pa). A solution of 7-oct-1-enyltrimethoxysilane (20 μl) and glacial acetic acid (20 μl) in methanol (4 ml) was passed through the column overnight (8–12 h) at 20 p.s.i. The capillary was subsequently rinsed with methanol and deionized water (1 h each, 20 p.s.i.). TEMED (8 μl) and aqueous ammonium persulfate (15% (w/v), 56 μl) were added to a solution of BCQ in deionized water (2% (v/v), 4 ml), and this solution was immediately rinsed through the column for 8 h (or overnight) at 20 p.s.i. The capillary was flushed with deionized water for 1 h and stored. Prior to use, the column was flushed with CZE buffer for 5–10 min.

2.3.2. APS coating

Columns were prepared as described by Moseley et al. [24]. Acid treatment was carried out with a 6 *M* solution of HCl for approximately 4 h and the column was purged with helium for 12 h at 300°C in a GC oven. Toluene was pumped through the column for 10 min, followed by a 2-h rinse with a 5% (v/v) solution of (3-aminopropyl)-trimethoxysilane in toluene. The column was flushed with toluene for 30 min and dried by purging with nitrogen at room temperature. Prior to use, the column was flushed with CZE buffer for approximately 10 min.

2.4. Nanosprayer tip construction

Construction of nanosprayers has been described in detail elsewhere [22]. Briefly, a fused-silica capillary, previously coated with BCQ, was cut into 10-cm lengths and tapered by suspending a metal weight (15 g) from one end of the capillary and melting the fused silica with the flame from a microwelding torch. The thinnest portion of the tapered column (up to 10 cm long and 2–5 μm O.D.) was trimmed to 2–3 cm, and inserted into a larger I.D. capillary (100 μm I.D.), and bent until the tapered end snapped. The tapered end was further sharpened by etching in a stirred solution of 48% HF for 15 min. During this process the internal volume of the capillary was rinsed with water (6 μl/min) to prevent the acid from etching the inner surface. After etching, the capillary surface was rinsed with water and purged with N_2 to remove any traces of HF.

The tapered tips were inserted into a 1.5-cm thick piece of foam at a 45° angle. The support foam was

positioned 5 cm from the gold target electrode on the stage of an Edwards 306A high vacuum coater. The exposed portion was sputter-coated with gold for 15–20 min by maintaining a voltage and current across the electrodes of 1.5 kV and 20 mA, respectively. The best results were achieved when a vacuum of $\leq 1\times10^{-5}$ Torr was obtained prior to coating. Typically 20–30 tips were sputter coated at one time.

After sputter coating, the gold coating on the tips was reinforced by electroplating. The gold-coated portion of the tip was covered with silver conductive paint to within 1 cm of the tapered tip to prevent the stirred and heated (60°C) gold-plating solution from removing the sputter-coated gold. To prevent blockage the capillary was continuously rinsed with deionized water (6 μl/min) during the plating process. A gold counter-electrode was used, and the plating current was maintained at 0.75 mA for 30 min.

2.5. Capillary zone electrophoresis

CZE–UV experiments were conducted using a P/ACE system (Beckman, Palo Alto, CA, USA) at a detection wavelength of 200 nm. Separation was achieved by applying 20 kV to the outlet end of an 87 cm×50 μm I.D. capillary. The background electrolyte was formic acid (0.1 or 1.0 *M*). The sample was introduced by pressure (35 mbar, 15 s), resulting in typical injection volumes of ~15 nl.

CZE–MS experiments were conducted using a Thermo CZE system (Thermo Capillary Electrophoresis, Franklin, MA, USA). Typically, the electrolytes used for nanospray CZE–MS were 0.1–1 *M* formic acid. Separations were achieved by applying −20 kV to the injection end of the column (1 m×50 μm I.D.) and ~2.5 kV to the nanosprayer tip. Samples were introduced by pressure (100 mbar, 6 s), resulting in ~27-nl injection volumes.

2.6. Mass spectrometry and nanoelectrospray interface

Nano-electrospray data were acquired using an API III$^+$ triple-quadrupole mass spectrometer (Perkin-Elmer Sciex, Concord, Ontario, Canada). A separate power supply (Glassman EH Series, Glassman, Whitehouse Station, NJ, USA) was used to provide the electrospray voltage. Mass spectra were acquired using stepped-orifice-voltage scanning as described by Carr and co-workers [14]. In the present work, the sampling-orifice voltage was maintained at 120 V during low-mass scanning (m/z 140–400) and 60 V during high-mass scanning (m/z 400–1600). Tandem mass spectra were acquired using dwell times of 2 ms per step of 0.5 Da in full-scan mode. A Macintosh Quadra 950 computer was used for instrument control, data acquisition and data processing.

The interface used in this work is shown in Fig. 1 and described in more detail elsewhere [22]. The nanosprayer tip was connected to the separation capillary using a commercially available column connector. The double-tapered ferrule used in this fitting was drilled to match the outer diameter of the capillary as closely as possible, as this ensures proper alignment of the tip with the capillary. Electrospray voltage was applied to the stainless steel support, and electrical contact with the CZE electrolyte exiting the gold-plated tip was ensured by the use of silver conductive paint. The contact with the stainless steel support also served to complete the electrophoretic circuit. Optimization of the interface was achieved by electro-infusion of a peptide standard (Leu-enkephalin, 10 μg/ml) dissolved in the electrolyte used for the separations described below.

3. Results and discussion

3.1. Optimization of separation conditions

The analysis of proteins and peptides by CZE using bare fused-silica capillaries is hampered by the adsorption of these analytes on the silanol surface [25,26]. This is especially true when using acidic buffers compatible with positive-ion electrospray, and can be overcome to some extent by using cationic coating agents. A common method for surface modification of capillaries for CZE–MS makes use of (3-aminopropyl)trimethoxysilane (APS) [24,27,28]. Recently we reported an alternative cationic coating, BCQ, for CZE analysis using acidic buffers [22].

The application of capillaries coated with either APS or BCQ is demonstrated for the separation of peptides obtained from mild acid hydrolysis of the

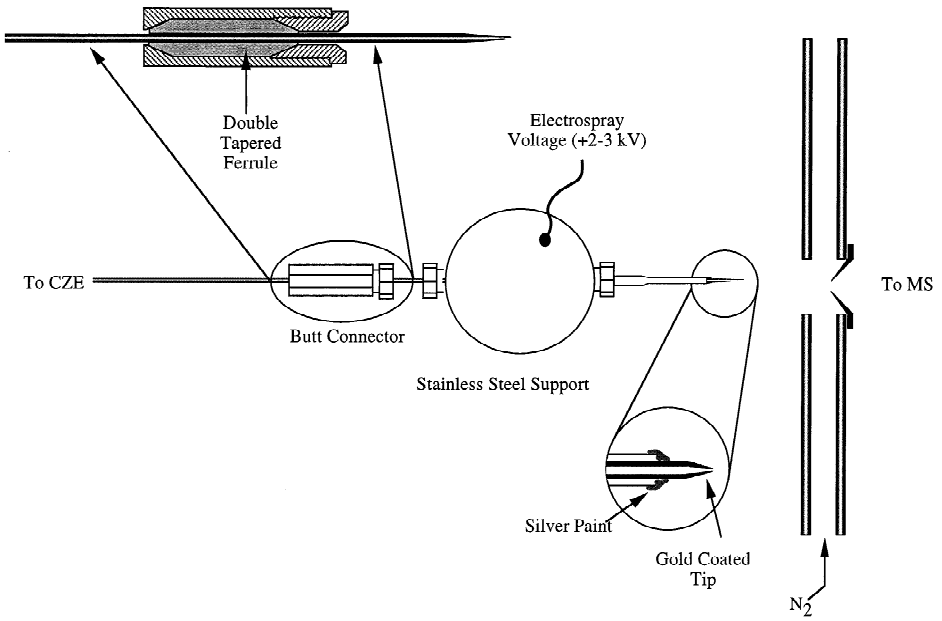

Fig. 1. Schematic representation of the CZE–MS nanoelectrospray interface.

α-chain from α-amylase inhibitor 1. This 76-amino acid glycopeptide has two potential sites for N-linked glycan, but no information on the nature or extent of glycosylation is known thus far. A more detailed structural investigation on the α- and β-chain complexes of *P. vulgaris* α-amylase inhibitor 1 will be presented separately. A comparison of CZE–UV electropherograms obtained for the analysis of peptides arising from the mild acid hydrolysis of this glycopeptide is presented in Fig. 2, and shows four electropherograms for APS and BCQ coatings each at two different concentrations of formic acid. Using 0.1 *M* formic acid, the separation performed using the BCQ coating (Fig. 2b) yielded improved resolution over that obtained using the APS coating (Fig. 2a). Electroosmotic flow (EOF) calculations at this electrolyte concentration gave values of 7.1×10^{-8} m^2 V^{-1} s^{-1} and 5.5×10^{-8} m^2 V^{-1} s^{-1} for the APS and BCQ coatings, respectively. Theoretical plate numbers (*N*, peak width at half height definition), calculated for the latest migrating component in Fig. 2a and 2b, gave *N* values of 185 000 and 322 000 for the APS and BCQ coatings, respectively. The improvement in performance is attributed to the decrease in electroosmotic flow. The analyte migrates in the direction opposite to that of the anodal electroosmotic flow, and the improvement in resolution comes as a result of the reduced zone velocity.

Electropherograms obtained using a 1 *M* formic acid separation buffer are shown in Fig. 2c and 2d for the APS and BCQ coated capillaries, respectively. In this instance the EOF measurements calculated for both coatings were similar (5.0×10^{-8} m^2 V^{-1} s^{-1}). When comparing results from a particular coating, the increase in acid strengths results in decreased EOF and improved peak resolution for both APS and BCQ coated capillaries. However, theoretical plate numbers calculated for the late migrating peak of each electropherogram were significantly different, with the APS coating giving a value of 220 000 while the BCQ coating gave a value of 505 000. Interestingly, closely migrating peaks such as those observed at approximately 12.6 min in Fig. 2d are more clearly resolved for the BCQ capillary than for the APS coating (Fig. 2c), achieved under similar separation conditions. In a separate experiment using CZE–MS (see following discussion), this set of peaks was identified as a series of high-mannose glycopeptides, and the heterogeneity observed here corresponds to the natural glycoform population at this particular site of attachment.

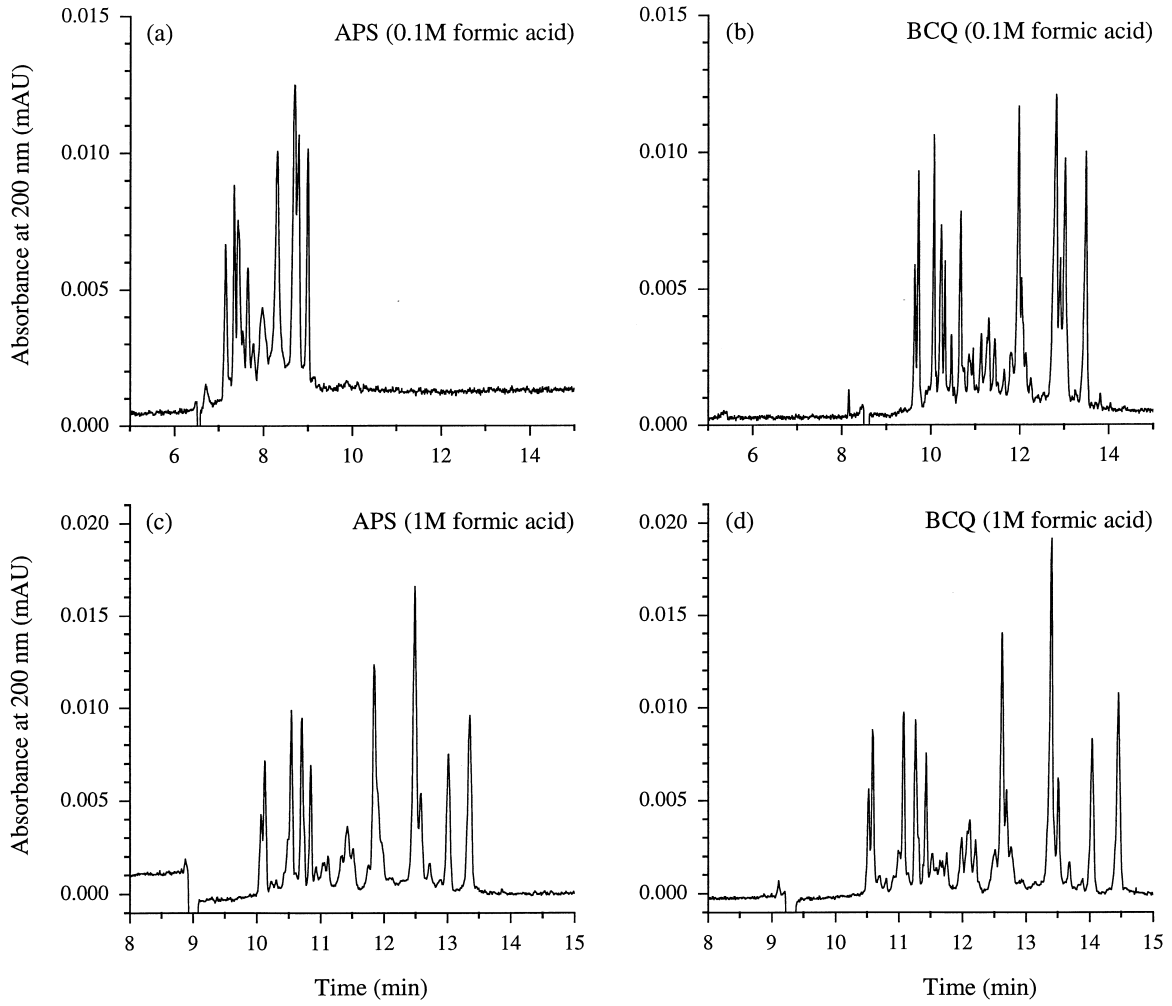

Fig. 2. Effects of capillary coatings and electrolyte buffers on the CZE–UV analysis of a mild acid hydrolysis of the α-chain from α-amylase inhibitor 1. Separation conducted using the following coatings and buffers: (a) APS, 0.1 *M* HCOOH; (b) BCQ, 0.1 *M* HCOOH; (c) APS, 1 *M* HCOOH; (d) BCQ, 1 *M* HCOOH. Conditions: injection of 15 nl on an 87 cm (total length)×50 μm I.D. coated capillary using reversed polarity (−20 kV).

The differences in separation performance of the BCQ- and APS-coated capillaries are mainly attributed to chemical structure and surface coverage of the two coatings. The structure of the BCQ comprises a quaternary amine acting as a permanent positive charge at the end of a 15-carbon alkyl chain, whereas a primary amine terminates the propyl chain of the APS coating. The overall charge imparted on the inner surface of the capillary will also depend on the ability to mask free silanol groups (pK_a=2.5). As the acid strength is increased the EOF is progressively reduced possibly through protonation of unreacted silanol groups. The short alkyl chain of the APS may not efficiently mask free silanol groups which are inevitably present, whereas the longer alkyl chain of the BCQ coating could provide a better surface coverage.

3.2. Identification of glycopeptides using CZE–MS

The optimization of the CZE–UV separation facilitated the selection of electrophoretic conditions

conducive to the analysis of glycoprotein digests using nanoelectrospray CZE–MS. Accordingly, separations of glycoprotein digests were usually conducted using the BCQ-coated capillary. To aid the identification of glycopeptides, a mixed-scan function was used to promote the in-source formation of selected oxonium ions under high-orifice-voltage conditions (120 V), while enabling detection of multiply protonated ions using low-orifice voltage (50 V). The analysis of the peptides arising from mild acid cleavage of the α-chain from α-amylase inhibitor 1 is presented in Fig. 3. The total ion electropherogram (TIE) corresponds to the injection of approximately 2 pmol of the original protein (Fig. 3a). The difference in resolution noted between Fig. 3a and the corresponding CZE–UV analysis (Fig. 2b) is attributed to several factors, including the use of a longer capillary (1 m), lower field strength (228 V cm^{-1}), and the relatively slow MS scan speed (3 s) used in the CZE–MS experiment. It is noteworthy that CZE–MS separations were also conducted using a 1.0 *M* HCOOH buffer and yielded improved resolution of the different glycoforms, though this resulted in longer analysis time and higher chemical noise contribution. The selection of the 0.1 *M* HCOOH buffer was thus preferred in all subsequent CZE–MS experiments.

Identification of glycopeptides in the TIE was achieved by extracting the *m*/*z* 204 ion electropherogram (Fig. 3b), corresponding to the GlcNAc oxonium ion generated by collision-induced dissociation in the orifice/skimmer region of the mass spectrometer. Resolution of closely related components is evident in the extracted ion electropherogram (Fig. 3b), including partial resolution of a series of four high-mannose glycopeptides centered at 19.0 min.

The microheterogeneity at a single site of glycosylation is more evident in the contour profile (Fig. 3c), where families of diagonal lines of negative slopes reflecting the concurrent changes in molecular mass and electrophoretic mobilities, are easily visualised. The first family of glycopeptides indicated by 1 in Fig. 3c, are spaced by *m*/*z* 54 consistent with triply protonated ions and corresponds to the peptide A_{1-20}, to which is bonded a variable oligosaccharide composed of $GlcNAc_2Man_x$ (where *x* ranges from three to six mannose residues). Based on the relative peak intensities, the predominant glycoform for this glycopeptide is $GlcNAc_2Man_6$. The peptide sequence (ATET-SFIIDAF**N**KTNLILQG) contains two asparagine residues, but only the first one (identified in bold) has the tripeptide sequon characteristic of an N-linked glycopeptide. It is interesting to note that the second and third series of doubly charged glycopeptide peaks at 16–17 min comprise the shorter-chain peptides A_{10-20} and A_{10-21} which display the same carbohydrate distribution.

The last two series of glycopeptide peaks centered at 19.0 and 21.0 min (labeled as 4 and 5 in Fig. 3c) correspond to the peptide fragments A_{54-76} and A_{64-76}, respectively. Both series of glycopeptides possess a variable oligosaccharide $GlcNAc_2Man_{6-9}$ where the predominant form is the Man_9 member. In this case the A_{54-76} peptide (STTGNVAS-FDTNFTMNIRTHRQA) contains a total of three asparagine residues, and only one encodes for a potential site of glycosylation.

3.3. Identification and characterization of N-linked glycopeptides using CZE–MS and CZE–MS–MS

The techniques of high-resolution CZE separation combined with nanoelectrospray MS detection, described above, were applied to the study of the seed lectin *Lotus tetragonolobus* (also referred to as *Tetragonolobus purpureas*). This lectin has been reported to exist as a 4:2:4 combination of three different subunits with molecular weights of 120, 58, and 117 kDa, respectively [29,30]. More recently, a sequence was reported for a single isolectin having a sub-unit molecular mass of approximately 26 000 Da by SDS–PAGE and 26 298 Da on the basis of the sequence determined by Edman degradation [31].

The mass spectrum generated by infusion of approximately 15 pmol of the intact lectin using the nanoelectrospray interface is shown in Fig. 4. The molecular mass profile calculated from the multiply charged ions of the mass spectrum is presented as an inset. The predominant peak has a molecular mass of 28 327 Da which is approximately 2 kDa higher than that calculated from the published protein sequence [31]. The mass difference observed here was first presumed to arise from the presence of up to two possible glycosylation sites. Further microheterogen-

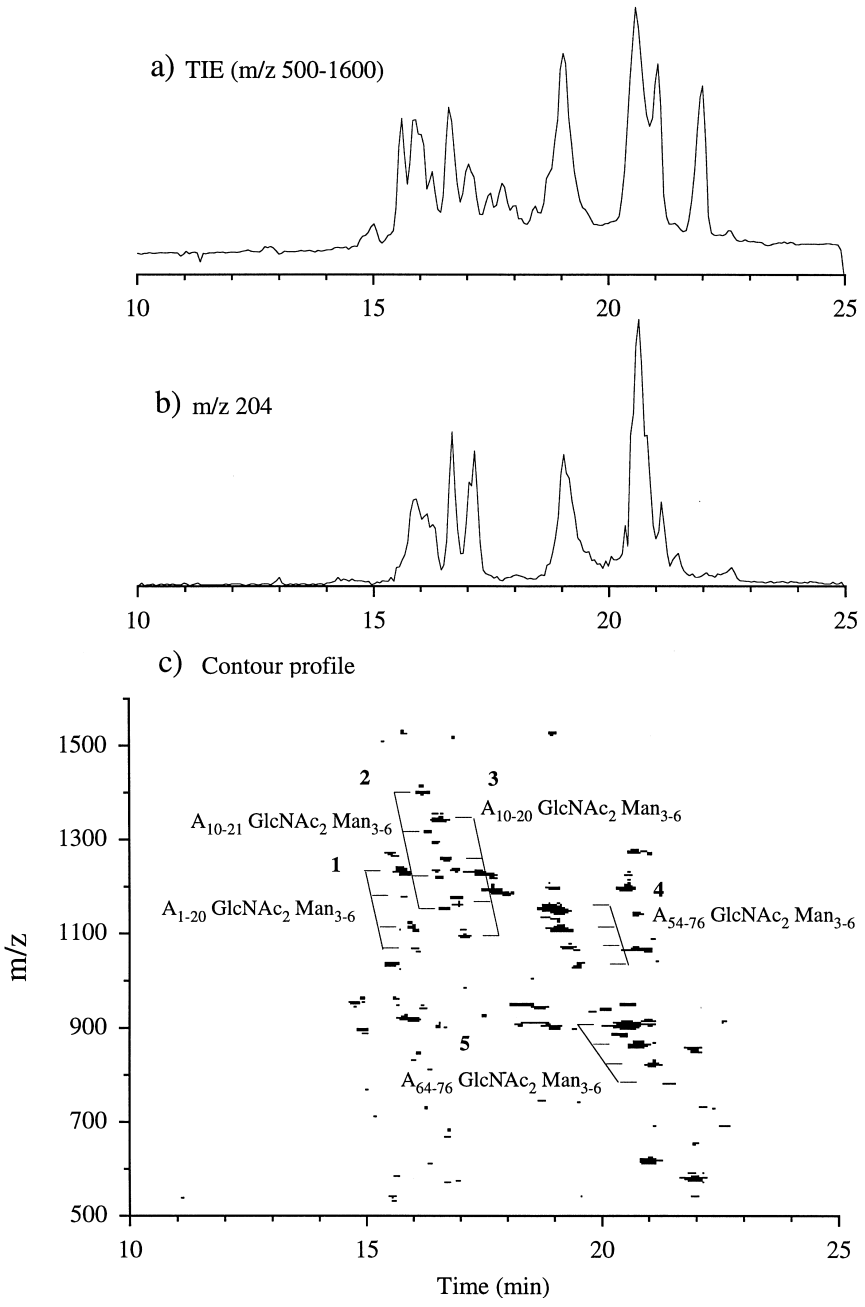

Fig. 3. Nanoelectrospray CZE–MS analysis of a mild acid hydrolysis of the α-chain from α-amylase inhibitor 1. (a) Total ion electropherogram (m/z 500–1600); (b) extracted ion for m/z 204; (c) contour profile of m/z vs. time. Conditions: injection of 27 nl (2 pmol of original digest) on a 1-m (total length)×50 μm I.D. BCQ-coated capillary using reversed polarity (−20 kV), and 0.1 *M* HCOOH.

eity could also be present in terms of addition or removal of carbohydrate residues. For example, a satellite peak at 28 476 Da would be consistent with the addition of a deoxyhexose (fucose) residue on the main glycoprotein shown in Fig. 4. However, other molecular species with mass differences of 114 Da

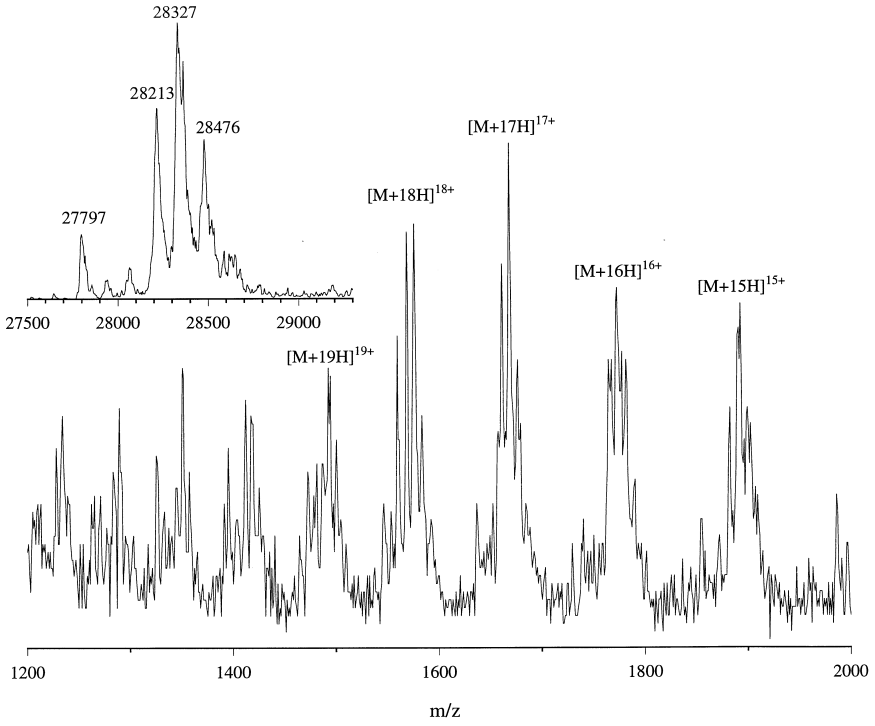

Fig. 4. Mass spectrum of *L. tetragonolobus* lectin obtained using nanoelectrospray. The reconstructed molecular mass is shown as an inset. Infusion of a total of 15 pmol of lectin in 0.1 *M* HCOOH).

were more difficult to explain, and further investigations were carried out to establish the glycoform distribution.

In order to identify the nature of the oligosaccharide(s) linked to this lectin, the glycoprotein was digested using trypsin and analyzed by nanoelectrospray CZE–MS. The TIE for the injection of approximately 3 pm of the original glycoprotein is shown in Fig. 5a. Selective identification of glycopeptides using the m/z 204 oxonium ion revealed two possible glycopeptides at approximately 16.9 and 17.5 min (Fig. 5c). It is noteworthy that earlier investigations by Carr and others have indicated that false positives for glycopeptides may occur using this HexNAc oxonium ion due to the large number of amino acid combinations coinciding with this m/z value [14,32]. More selective identification of glycopeptides can be accomplished using two or more oxonium ions. In this instance, extracted ions for m/z 163 (hexose, Fig. 5b) and m/z 366 (GlcNAc-hexose, Fig. 5d) were used along with m/z 204 to confirm the presence of one glycopeptide (17.5 min) while rejecting a possible false positive (16.9 min). It is noteworthy that peptides containing N-terminal GE or C-terminal GF amino acid segments could lead to b_2 or y_2 fragment ions at m/z 204. The identity of the false positive at 16.9 min is not known at present but could possibly be explained by the occurrence of a peptide arising from an unspecific cleavage or from a C-terminal amino acid extension leading to additional peptides (see following discussion).

The extracted mass spectrum from the peak identified as a glycopeptide at 17.5 min in Fig. 5 is presented in Fig. 6a. This spectrum was acquired using a normal orifice voltage of 50 V. The potential drop between the orifice and the front rods (Q0 or ion guide) does not then provide sufficient energy to induce fragmentation by collision-induced dissociation in this relatively high-pressure region of the vacuum chamber. The spectrum contains $[M+2H]^{2+}$, $[M+3H]^{3+}$, and $[M+4H]^{4+}$ ions and correspond to a calculated molecular mass of 3372 Da.

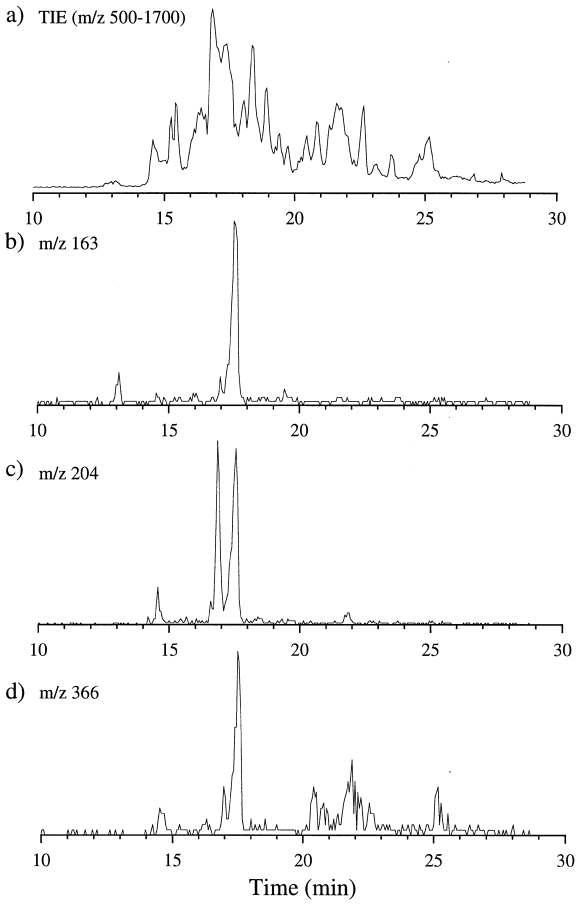

Fig. 5. Nanoelectrospray CZE–MS analysis of a tryptic digest of *L. tetragonolobus* lectin. (a) Total ion electropherogram (m/z 500–1800); (b) extracted ion profile for m/z 163; (c) m/z 204; and (d) XIE m/z 366. Conditions: 1.5-pmol injection of original digest on a 1-m (total length)×50 μm I.D. BCQ-coated capillary using reversed polarity (−20 kV), and 0.1 *M* HCOOH.

Interestingly, closely migrating peaks spaced by m/z 48 and 36 from the predominant $[M+3H]^{3+}$ and $[M+4H]^{4+}$ species may correspond to an additional glycopeptide containing an extra fucose residue. Indeed, a peptide fragment of molecular mass of 3518 Da was identified on the fronting edge of the peak at 17.5 min, thereby suggesting the presence of a mixed population of fucosylated/defucosylated glycopeptides.

Analysis of the same digest, using identical separation conditions, except for the use of a higher orifice voltage (120 V) yielded the spectrum shown in Fig. 6b, and demonstrate fragmentation of the glycopeptide prior to mass analysis. The corresponding mass spectrum is obviously more complicated than that shown in Fig. 6a, but provided valuable information concerning the nature of the oligosaccharide appended to the peptide backbone. For example, the most abundant ion in Fig. 6b is observed at m/z 1276, and was tentatively assigned to a doubly charged peptide fragment plus a GlcNAc residue. Previous investigations using low-energy tandem mass spectrometry have indicated that cleavage at the glycosidic bond between two GlcNAc residues is commonly observed for N-linked glycopeptides [33]. The molecular mass of the corresponding deglycosylated peptide would be 2347 Da. The sequence of this peptide contains the consensus sequon Asn_4–Tyr–Thr_6 and the calculated mass of the tryptic peptide containing this sequence is 1134 Da. The mass of the peptide T_{1-21} when cleaved at the next available site is 2347 Da (VSFNYTEFKDDGSLILQGDAK), in close agreement with that observed in Fig. 6b. The close proximity of an adjacent aspartic acid residue at D_{10} prevented the formation of the corresponding tryptic peptide, thereby resulting in a larger proteolytic fragment.

Analysis of the spectrum produced using a high orifice voltage (Fig. 6b) allows tentative assignment of the carbohydrate composition. A series of doubly charged fragment ions is present in the spectrum, corresponding to additional GlcNAc and hexose residues from the $[peptide+GlcNAc]^{2+}$ fragment ion. Based on the spectra shown in Fig. 6, the mass of the oligosaccharide attached to T_{1-21} was calculated to be 1025 Da. The conserved pentasaccharide ($GlcNAc_2Man_3$) of N-linked glycopeptide has a residue mass of 892 Da which is 133 Da shorter than the expected mass for the oligosaccharide, a difference which could be accounted for by a pentose residue (xylose). The additional component observed in Fig. 6a would thus correspond to the tryptic glycopeptide T_{1-21} to which is attached oligosaccharide structure $GlcNAc_2Man_3$–Xyl–Fuc.

Additional confirmation of the structural identity of this tryptic glycopeptide was obtained using online CZE–MS–MS. Structural features of the glycopeptide were probed using low-energy collision activation of the multiply protonated precursor ions. The CZE–MS–MS spectrum of the $[M+3H]^{3+}$ ion of the tryptic peptide at m/z 1125 (Fig. 6a) is shown

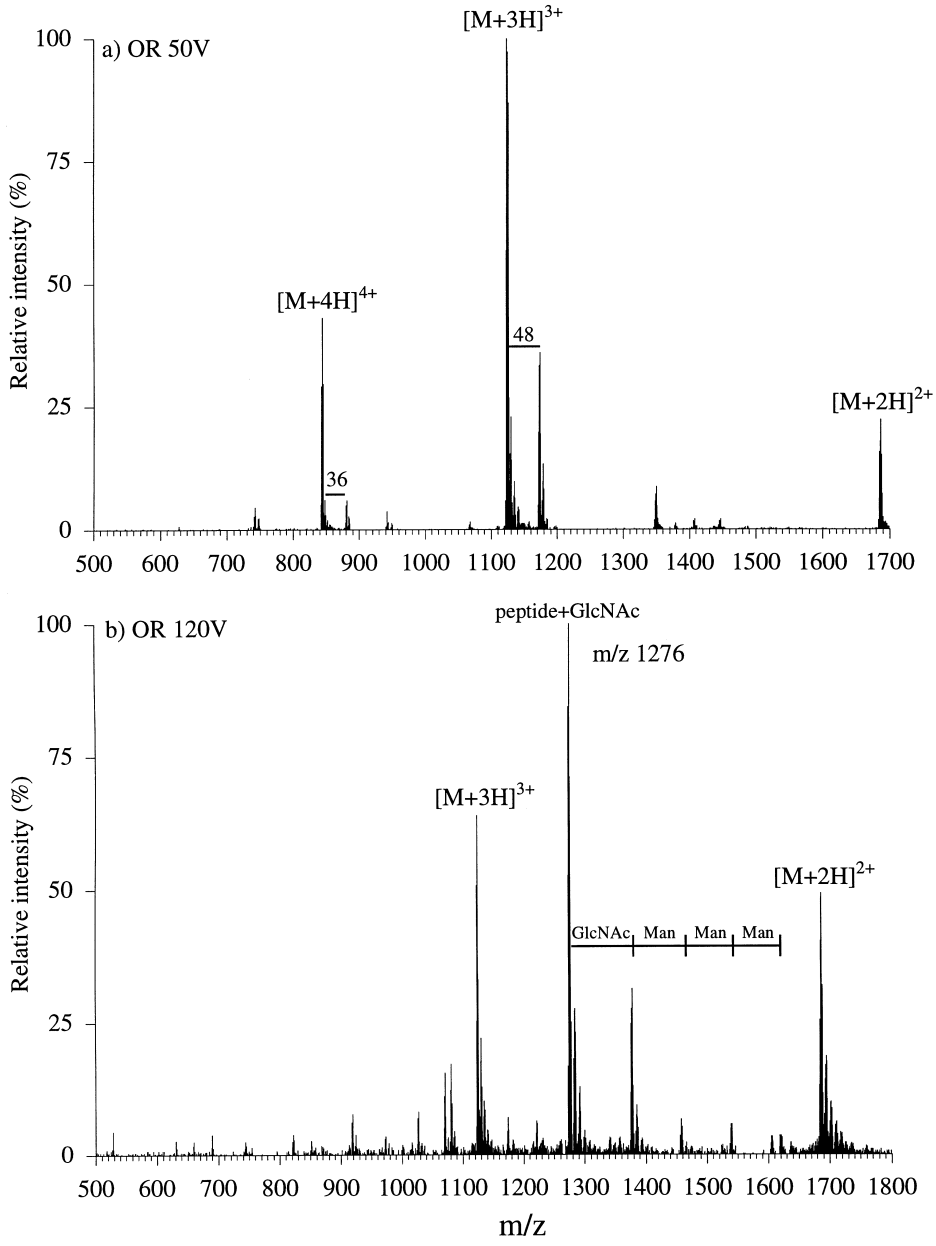

Fig. 6. Extracted mass spectra from the nanoelectrospray CZE–MS analysis of the tryptic digest of *L. tetragonolobus* lectin using an orifice voltage of (a) 50 V (peak migrating at 17 min in Fig. 5a) and (b) 120 V (obtained from a separate CZE–ES-MS analysis). Conditions as for Fig. 5.

in Fig. 7a, and was produced from the injection of 1.5 pmol of original protein. The appearance of the spectrum is similar to that of the high-orifice full-scan spectrum (Fig. 6b), in that the most abundant ions are the $[M+3H]^{3+}$ ion of the intact glycopeptide and the $[M+2H]^{2+}$ ion of the peptide+GlcNAc. However, the 2+ and 3+ fragment ions arising from the cleavage of carbohydrate residues

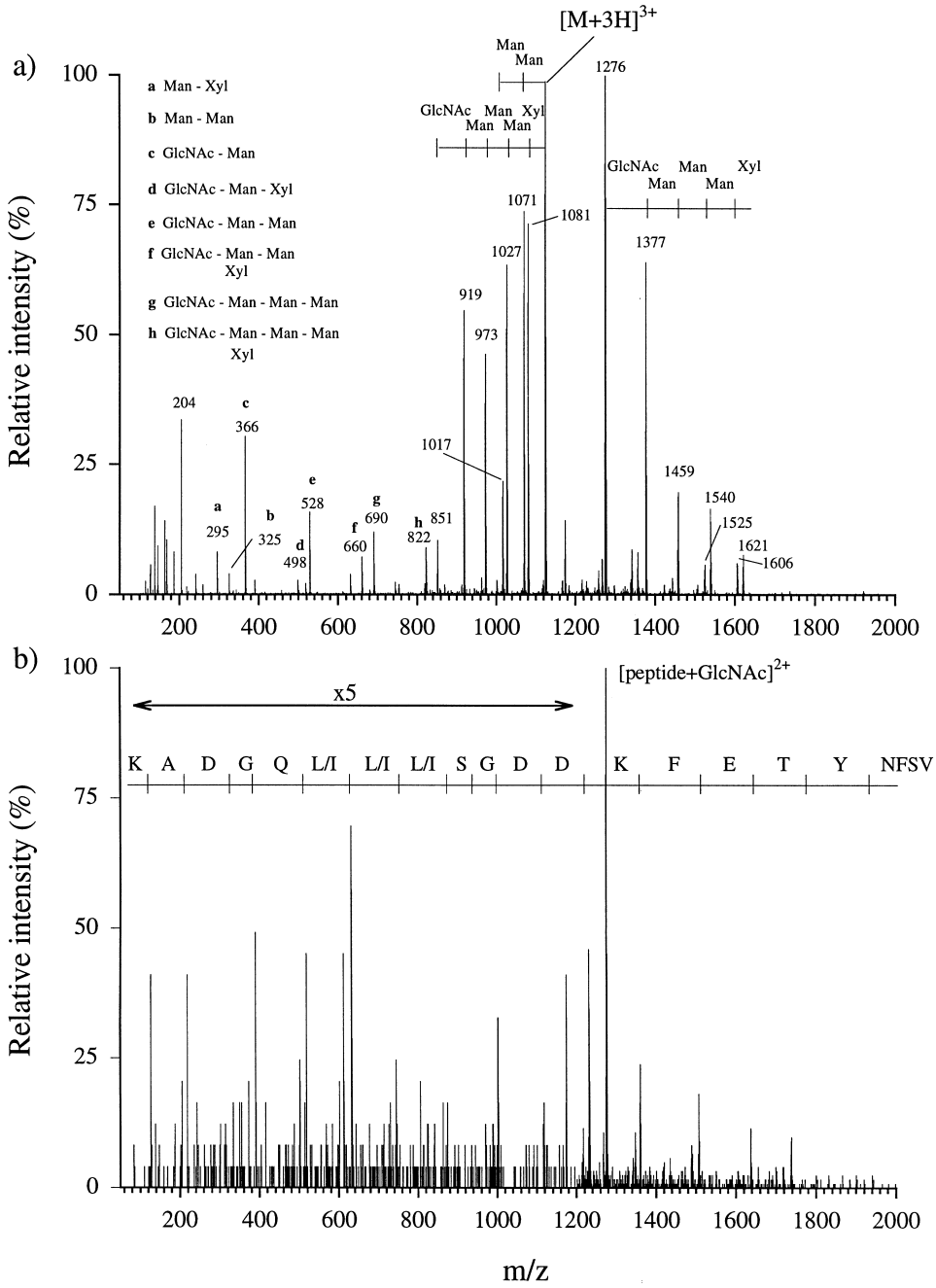

Fig. 7. Nanoelectrospray CZE–MS–MS analysis of a glycopeptide from the tryptic digest of *L. tetragonolobus* lectin. (a) Product ion scan of m/z 1125 corresponding to the $[M+3H]^{3+}$ glycopeptide ion shown in Fig. 6a. (b) Product ion scan of m/z 1276 corresponding to the $[peptide+GlcNAc]^{2+}$ fragment ion shown in Fig. 6b obtained at an orifice voltage 120 V. Conditions as for Fig. 5 except that the separation voltage was decreased to −5 kV at 16 min; argon target gas; collision gas thickness, 3.5×10^{-15} atoms cm^{-2}, collision energy (laboratory frame of reference) of 75 eV for (a) and 60 eV for (b). Fragment ions identified correspond to y-type ion series.

from the precursor ion are significantly more abundant than in the high-voltage orifice experiment (Fig. 6b). From this spectrum the structure of the oligosaccharide is assigned as $GlcNAc_2Man_3$ with a pentose sugar attached to the central mannose residue. The location of the pentose residue is based on the ion pairs associated with loss of either mannose or pentose and from the oligosaccharide fragment ions observed below m/z 900 (Fig. 7a). The oxonium ions at m/z 163, 204 and 366 used for selective detection of the glycopeptide in the CZE–MS analysis of the tryptic digest of the lectin are clearly observed in Fig. 7a. These ions, along with those at m/z 295, 325, 498, 528, 660, 690 and 822 were consistent with the structure of the oligosaccharide described above.

One of the limitations of the low-energy spectra generated by triple quadrupole instruments is the lack of information about the peptide backbone of the glycopeptide. The collision energy is dissipated through cleavage of the most labile bonds, which in the case of glycopeptides are the glycosidic linkages. Observation of highly abundant fragment ions corresponding to the peptide backbone plus GlcNAc in the high orifice full scan data of glycopeptides prompted the investigation of these ions as possible precursors for MS–MS studies of peptide sequences. In the case of the *L. tetragonolobus* lectin, the fragment ion at m/z 1276 $[peptide+GlcNAc]^{2+}$ served as the precursor. This ion was produced as a first-generation fragment ion by CID in the orifice/skimmer region of the mass spectrometer and was subjected to further CID in the collision cell. The spectrum generated by this technique is shown in Fig. 7b. The assignment of the y series ions was in excellent agreement with the sequence published previously [31]. Liu et al. reported an approach similar to this using microcolumn LC–MS–MS, but considered the peptide plus GlcNAc ion to be an artifact of the ionization process and did not attempt to purposely exploit these ions [34].

It is noteworthy that the work described above confirmed the occurrence of only one site of glycosylation, with minor heterogeneity involving the incorporation of an additional fucose residue. The corresponding oligosaccharide would increase the protein molecular mass by 1044 to 27 342 Da. The significant mass difference noted between the published sequence and the results of the present work is possibly accounted for by variation in the gene sequence or by the nature of the seeds extracted from different samples of *L. tetragonolobus*. Indeed a single potential site of glycosylation was expected from the reported sequence [31] and no additional glycopeptide was observed in experiments described above. Since the tryptic peptide expected from the N-terminus of this glycoprotein was confirmed in this study, one possible explanation for the present findings could be the occurrence of truncations at the C-terminus. Previous investigations on recombinant and natural plant lectins have highlighted that C-terminal proteolytic processing often results in heterogeneity and can be a major contributor to the appearance of isolectin forms [35].

3.4. Analysis of κ-casein, a complex O-linked glycoprotein

The established method of Edman degradation for the study of O-glycosylation is only useful for those sites that are extensively modified (80–100%). This is due to the poor recovery of glycosylated anilinothiazolinone-amino acids in the solvents typically used in automated sequencers. The use of solid-phase Edman degradation has overcome these limitations to some extent [36]. In the present study, the use of CZE nanoelectrospray–MS was investigated for the study of O-glycosylation sites especially in instances where only partial glycosylation occurs.

The TIE for the CZE–MS analysis of 5 pmol of a Glu-C digest of the rennin fragment of κ-casein, an O-glycosylated milk protein, is shown in Fig. 8a. This glycoprotein is known to have N-acetylneuramic acid (Neu5Ac) residues as part of the oligosaccharide structure, and selective identification of the glycopeptides is shown in Fig. 8b. Using a mixed-scan function to generate oxonium ions for the Neu5Ac (m/z 292), or in this instance Neu5Ac minus water (m/z 274), provides a higher degree of selectivity. The Neu5Ac residues are known to be acid labile, however the analysis using 0.1 *M* formic acid did not give rise to noticeable degradation. The contour profile for the analysis of the digest is shown in Fig. 8c and reveals the complexity of the sample.

An alternative approach to the selective identifica-

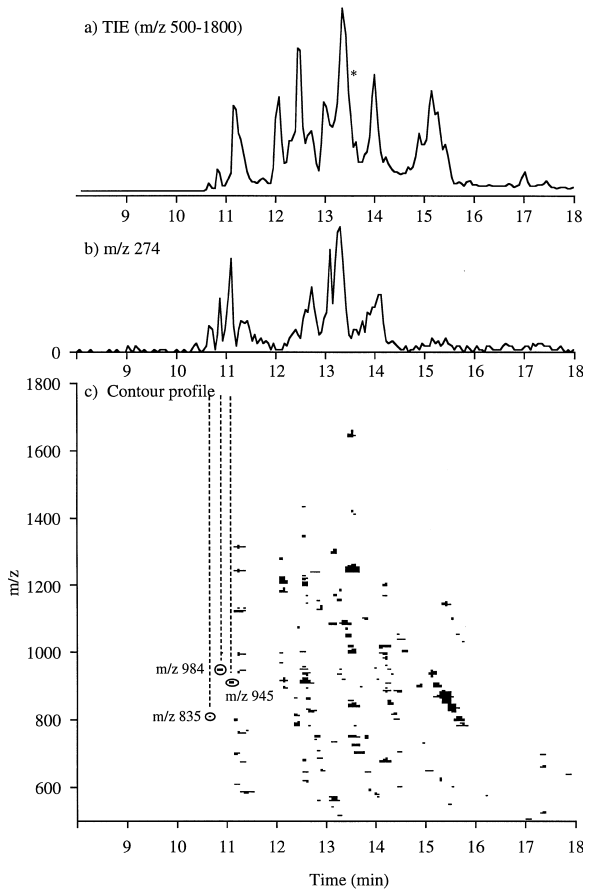

Fig. 8. Analysis of Glu-C digest of κ-casein using nanoelectrospray CZE–MS. (a) Total ion electropherogram (m/z 500–1800); (b) extracted ion electropherogram for m/z 274 obtained at an orifice voltage of 120 V; (c) contour profile of m/z vs. time. Conditions: 5-pmol injection of original digest on a 1-m (total length)×50 μm I.D. BCQ-coated capillary using reversed polarity (−20 kV), and 0.1 *M* HCOOH. The asterisk indicates the non-glycosylated peptide $S_{36}TVATLE_{42}$.

tion of the glycopeptides is to use precursor ion scanning. In this method, a normal orifice voltage is used and the peptides are fragmented in the r.f.-only quadrupole collision cell of the mass spectrometer. The third quadrupole is set to transmit only m/z 274, a fragment ion specific to Neu5Ac as discussed above. The first quadrupole is scanned over the mass range of interest (m/z 500–1500), and the corresponding spectra display only precursor ions for the selected transition. The TIE for the analysis of the κ-casein Glu-C digest using the precursor ion scanning for m/z 274 is shown in Fig. 9a, and the resulting electropherogram is similar to the stepped-orifice scanning profile shown in Fig. 8b. However, the peaks in the precursor-ion scan contain information on the molecular masses of the glycopeptides without interference from other nonglycosylated peptides of this digest. Examples of the mass spectra extracted from the first three peaks are shown in Fig. 9b–c. The later peaks are due to higher-molecular-weight components resulting from incomplete digestion of the glycoprotein.

The composition of the carbohydrate component of the glycopeptide can be obtained using CZE–MS–MS as discussed above. These experiments were carried out on the digested O-linked glycoprotein, using m/z 835 and 984 as precursors. The resulting fragment ion spectra are presented in Fig. 10 and clearly show abundant fragment ions at m/z 274 and 292, corresponding to Neu5Ac. These spectra also

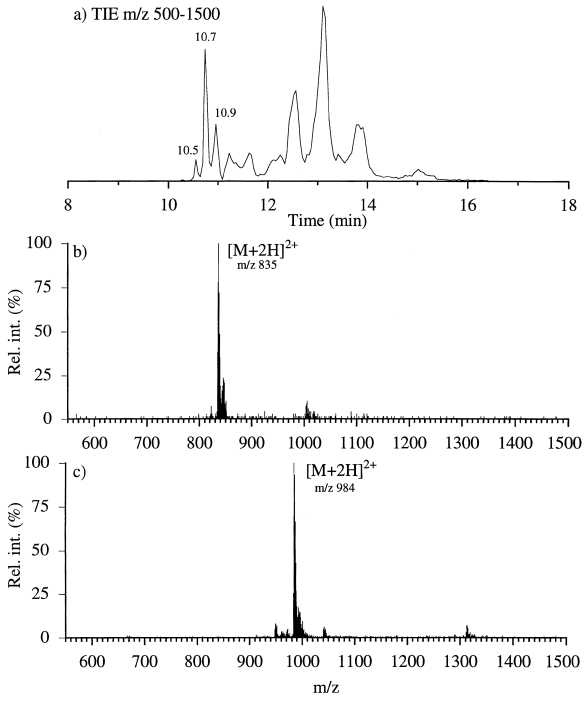

Fig. 9. Analysis of sialylated glycopeptides from κ-casein using precursor ion scanning for m/z 274. (a) Total ion electropherogram of precursor ion (m/z 500–1500); extracted mass spectra at (b) 10.5 and (c) 10.7 min. Separation conditions as for Fig. 8, except: argon target gas; collision gas thickness, 3.5×10^{-15} atoms cm^{-2}, collision energy of 60 eV (laboratory frame of reference).

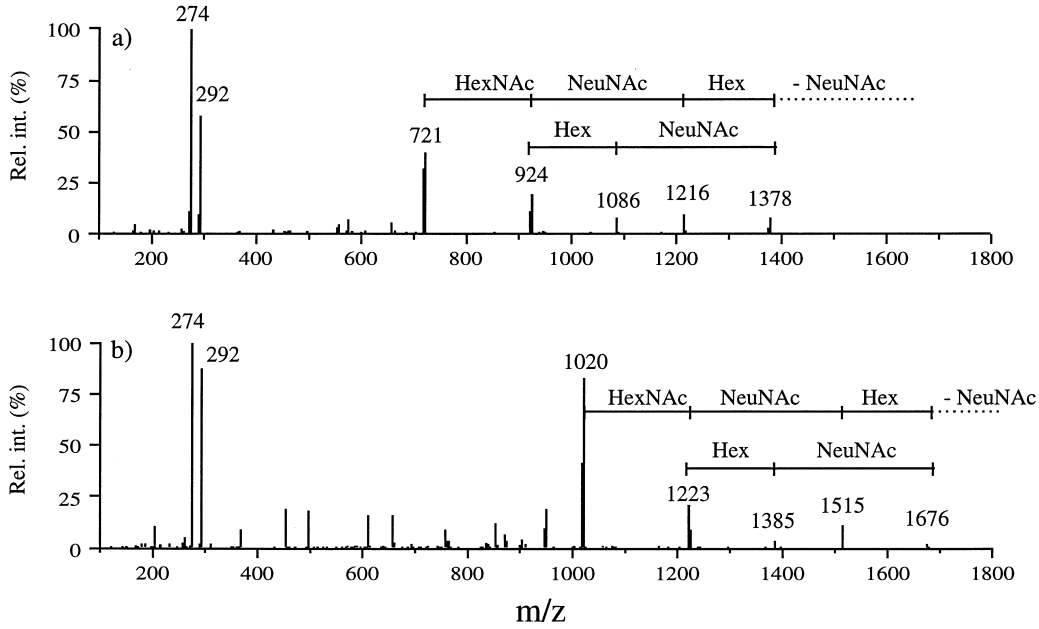

Fig. 10. Nanoeletrospray CZE–MS–MS analysis of O-linked glycopeptides from Glu-C digest of κ-casein. (a) Product ion scan of m/z 835; (b) product ion scan of m/z 984. Conditions as for Fig. 9, except that the separation voltage was decreased to −5 kV at 10 min.

show that the initial cleavage of a Neu5Ac residue is followed by loss of either a hexose or another Neu5Ac. This observation is consistent with the presence of a branched oligosaccharide and reveals that one of the Neu5Ac residues is attached to the core HexNAc residue. If both Neu5Ac sugars were attached to the hexose, the ions at m/z 1216 and 1515 in Fig. 10a and 10b, respectively would not be expected. Also evident in these spectra are the fragment ions for the naked peptides at m/z 721 and 1020, in Fig. 10a and 10b, respectively. Comparison of these values with the predicted molecular masses for the digest fragments of κ-casein reveals that the sequence of the peptides are $S_{36}TVATLE_{42}$ (M_r 719.8) and $A_{33}VESTVATLE_{42}$ (M_r 1019.1). The second peptide arose from a skipped cleavage at E_{35}. According to previously published sequence analysis of κ-casein, T_{37} is expected to be glycosylated [37]. The non-glycosylated peptide, $S_{36}TVATLE_{42}$, is also present in the peptide map of this glycoprotein, and is marked with an asterisk in Fig. 8a. No signal was detected for the non-glycosylated peptide corresponding to the skipped cleavage site, suggesting that the presence of the oligosaccharide may hamper the enzymatic cleavage at Glu_{35}. In the present case, the non-glycosylated peptide is significantly more abundant than the corresponding glycosylated peptide. However, the sensitivity of the present CZE–MS techniques enabled detection of both glycosylated and non-glycosylated peptides.

As emphasized above, the low-energy CZE–MS–MS analysis of glycopeptides provided information only on the oligosaccharide structure and composition, but failed to generate peptide sequence fragments. The identification of sequence segments could only be made by matching the calculated molecular masses with those expected from the reported sequence when available. However, since there is no consensus sequence for predicting sites of O-glycosylation, knowing the sequence of the peptide from cDNA does not help in assigning the actual location of the oligosaccharide on the peptide. Further complications arose from the fact that both threonine and serine can be glycosylated, and in the present example there are three possible sites for attachment of the oligosaccharide.

The formation of first-generation fragment ions to produce the peptide+HexNAc ion, which are subsequently analysed by MS–MS, can be used to provide additional information on the peptide sequence. This is demonstrated in Fig. 11 for the tandem mass spectrum of m/z 924 (Fig. 10a) obtained from combined CZE–MS–MS. Fragmentation of the peptide occurs to produce the well-defined series of y and b ions. Loss of water from the b series ions is also a common fragmentation pathway when an acidic residue (glutamic acid) is located at the C-terminus of the peptide (S_{36}TVATLE$_{42}$). Notably absent from the spectrum are the b_2 and y_6 ions at m/z 189 and 633, respectively. The absence of these fragment ions might be coincidental as the corresponding fragment ions containing the HexNAc residue were not observed in this MS-MS spectrum. Further investigations are in progress to unambiguously identify sites of glycosylation in O-linked glycopeptides.

4. Conclusions

The application of CZE to the analysis of complex mixtures resulting from enzymatic and chemical digests of glycoproteins has been demonstrated. The use of BCQ-modified capillaries with dilute formic acid electrolyte provides high resolution of glycopeptides while maintaining compatibility with MS detection. The use of CZE combined with nanoelectrospray mass spectrometry enabled identification of glycopeptides using low picomole injections of original protein digests. Stepped-orifice voltage scanning methods and precursor-ion scanning generated ions which are specific for the carbohydrate moieties of interest. These techniques facilitate the location of the glycopeptides in the CZE–MS analysis of proteolytic digests.

The combination of CZE with on-line tandem mass spectrometry generated structural information restricted to the oligosaccharides appended to the

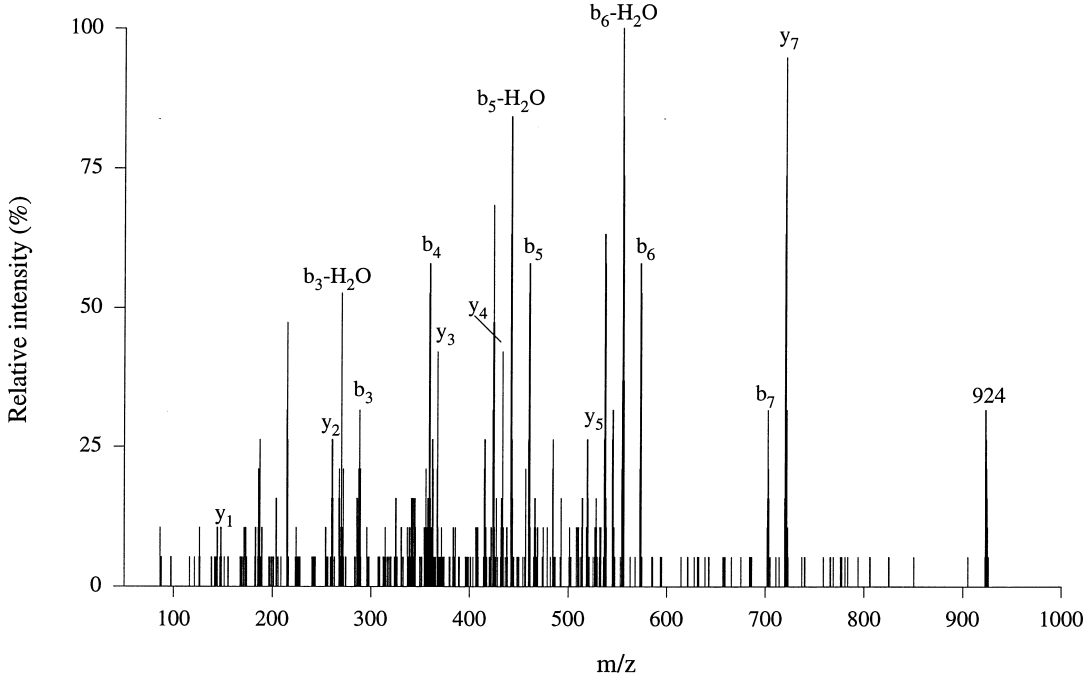

Fig. 11. Product ion spectrum of precursor m/z 924 corresponding to the [peptide+GalNAc]$^+$ ion identified in Fig. 10a. Conditions as for Fig. 10, except for a collision energy of 32 eV (laboratory frame of reference). The fragment ions indicated correspond to those of peptide backbone minus GalNAc.

peptide backbone. By promoting the formation of first-generation fragment ions in the orifice/skimmer region, peptide sequence analysis could be obtained by conducting tandem mass spectrometric experiments on the fragment ion corresponding to [peptide+GlcNAc]. The combination of these experiments enabled characterization of both carbohydrate and peptide structures. Identification of glycopeptides and characterization of site heterogeneity were described for a number of N- and O-linked glycoproteins and provided valuable structural information using low picomole sample loadings. These techniques should provide a powerful tool for the structural analysis of glycoproteins, particularly in instances where sample availability is limited.

Acknowledgements

The authors gratefully acknowledge the technical assistance of D. Watson (IBS, Ottawa), Dr. M. Chrispeels (Dept. of Biology, University of California, San Diego, CA, USA) for the gift of α-amylase inhibitor 1 and Drs. R.K. Boyd and N.M. Young for valuable discussions.

References

[1] R.A. Dwek, Chem. Rev. 96 (1996) 683–720.
[2] R.B. Parekh, A.G.D. Tse, R.A. Dwek, A.F. Williams, T.W. Rademacher, EMBO J. 6 (1987) 1233.
[3] C.F. Goochee, M.J. Gramer, D.C. Andersen, J.B. Bahr, J.R. Rasmussen, in: P. Todd, K. Sikdar, M. Bier (Eds.), Frontiers in Bioprocessing II, American Chemical Society, Washington, DC, 1992, pp. 199–240.
[4] R. Kornfeld, S. Kornfeld, Annu. Rev. Biochem. 54 (1985) 631.
[5] H.A. Kaplan, J.K. Welply, W.J. Lennarz, Biochim. Biophys. Acta 906 (1987) 161.
[6] R.D. Marshall, Biochem. Soc. Symp. 40 (1974) 17.
[7] Y. Gavel, G. von Heijne, Protein Eng. 3 (1990) 433.
[8] S.H. Shakin-Eshleman, S.L. Spitalnik, L. Kasturi, J. Biol. Chem. 271 (1996) 6363.
[9] K. Nehrke, F.K. Hagen, L.A. Tabak, J. Biol. Chem. 271 (1996) 7061.
[10] Volume 230 of Methods in Enzymology is dedicated to techniques in Glycobiology.
[11] W.J. Richter, D.R. Mller, B. Domon, Methods Enzymol. 193 (1990) 607.
[12] R.B. Parekh, Methods Enzymol. 230 (1994) 340.
[13] S.A. Carr, J.R. Barr, G.D. Roberts, K.R. Anumula, P.B. Taylor, Methods Enzymol. 193 (1990) 501.
[14] M.J. Huddleston, M.F. Bean, S.A. Carr, Anal. Chem. 65 (1993) 877.
[15] S.A. Carr, M.J. Huddleston, M.F. Bean, Protein Sci. 2 (1993) 183.
[16] J.F. Kelly, S.J. Locke, L. Ramaley, P. Thibault, J. Chromatogr. A 720 (1996) 409.
[17] R.L. Chen, D.S. Burgi, Anal. Chem. 64 (1992) 1046.
[18] D.S. Burgi, R.L. Chen, Anal. Chem. 63 (1991) 2042.
[19] S.J. Locke, P. Thibault, Anal. Chem. 66 (1994) 3436.
[20] A.J. Tomlinson, S. Naylor, J. High Resol. Chromatogr. 18 (1995) 384.
[21] J.F. Kelly, L. Ramaley, P. Thibault, Anal. Chem. 69 (1997) 51.
[22] K.P. Bateman, R.L. White, P. Thibault, Rapid Commun. Mass Spectrom. 11 (1997) 307.
[23] C.A. Zittle, J.H. Custer, J. Dairy Sci. 46 (1963) 1183.
[24] M.A. Moseley, L.J. Deterding, K.B. Tomer, J.W. Jorgenson, Anal. Chem. 63 (1991) 109.
[25] R.M. McCormick, Anal. Chem. 60 (1988) 2322.
[26] X.W. Yao, D. Wu, F.E. Regnier, J. Chromatogr. 636 (1993) 21.
[27] D.R. Goodlett, J.H. Wahl, H.R. Udseth, R.D. Smith, J. Microl. Sep. 5 (1993) 57.
[28] J.R. Perkins, K.B. Tomer, Anal. Chem. 66 (1994) 2835.
[29] A.J. Kalb, Biochim. Biophys. Acta 168 (1968) 532.
[30] S. Blumberg, J. Hildesherim, J. Yariv, K.J. Wilson, Biochim. Biophys. Acta 264 (1972) 171.
[31] Y. Konami, K. Yamamoto, T. Osawa, FEBS Lett. 268 (1990) 281.
[32] M. Wilm, G. Neubauer, M. Mann, Anal. Chem. 68 (1996) 527.
[33] J.J. Conboy, J.D. Henion, J. Am. Soc. Mass Spectrom. 3 (1992) 804.
[34] J. Liu, K.J. Volk, E.H. Kerns, S.E. Klohr, M.S. Lee, I.E. Rosenberg, J. Chromatogr. 632 (1993) 45.
[35] N.M. Young, D.C. Watson, M. Yaguchi, R. Adar, R. Arango, E. Rodriguez-Arango, N. Sharon, P.K.S. Blay, P. Thibault, J. Biol. Chem. 270 (1996) 2563.
[36] A.A. Gooley, B.J. Classon, R. Marschalek, K.L. Williams, Biochem. Biophys. Res. Commun. 178 (1991) 1194.
[37] A. Pisano, N.H. Packer, J.W. Redmond, K.L. Williams, A.A. Gooley, Glycobiology 4 (1994) 837.